

OPEN SET FACE FORGERY DETECTION VIA DUAL-LEVEL EVIDENCE COLLECTION (SUPPLEMENTARY MATERIALS)

Anonymous authors

Paper under double-blind review

A DATASET SETUP DETAILS

Table 1: Forgery configuration of each fake category in our OSFFD setting. This table details the specific deepfake forgeries included in each fake category. Certain forgeries are used in both the training and testing phases, while others are reserved exclusively for testing.

	FS	FR	EFS	FE	SM
Train & Test	FSGAN, FaceSwap, SimSwap, InSwapper, BlendFace	FOMM, FS.vid2vid, Wav2Lip, MRAA, OneShot	VQGAN, HStyleGAN-XL, SD-2.1, StyleGAN2, StyleGAN3	\	\
Test Only	UniFace, MobileSwap, e4s, FaceDancer, DeepFaceLab	LIA, TPSMM, HyperReenact, DaGAN, SadTalker, MCNet, PIRender, HeyGen	PixArt-alpha, MiniJourney6, DDPM, WhichisReal, RDMM, DIT-XL/2, SIT-XL/2	StarGAN, StarGANv2, e4e, CollabDiff, StyleCLIP	DeepFakes-StarGAN-Stack, StarGAN-BlendFace-Stack

Here, we provide the data configuration details about our setup in our Open Set Face Forgery Detection (OSFFD) experiments. We utilize the DF40 (Yan et al., 2024) dataset, which comprises four fake categories, and further incorporate two Stacked Manipulation forgeries from the ForgeryNet benchmark (He et al., 2021), resulting in five distinct fake categories in total. Specifically, the five fake categories are: Face Swapping (FS), Face Reenactment (FR), Entire Face Synthesis (EFS), Face Editing (FE), and Stacked Manipulation (SM). Due to the limited amount of fake data available for FE and SM, these two categories are treated as novel fake categories. The remaining categories FS, FR, and EFS are considered as either seen or unseen categories across different experimental configurations. As outlined in the main paper, we initially adopted a leave-one-out strategy, in which one of the three categories was withheld during training and regarded as an unseen category during testing. In a subsequent setting, all three categories (FS, FR, and EFS) were included as known classes, while FE and SM were used as novel fake categories during evaluation. During the training phase, the data consists of faces from real class and known fake categories, whereas the testing phase additionally includes samples from novel fake categories.

Since the number of forgeries varies across the fake categories FS, FR, and EFS, we select five forgeries from each category for use in both training and testing, while reserving the remaining forgeries for testing only. We show the forgery configuration in Table 1. For detailed information on the methods included in FS, FR, EFS, and FE, along with the corresponding data quantities, sources, and sub-types, please refer to Table 2 in the DF40 paper (Yan et al., 2024). The methods categorized under SM can be found in Figure 3 of the ForgeryNet benchmark paper (He et al., 2021). We followed the original training and testing splits for each specific deepfake forgery and performed dataset balancing by randomly selecting the largest possible subset such that each fake category contained an equal number of samples, and the overall number of real and fake face images was balanced.

B IMPLEMENTATION DETAILS

Network Modules. Our Dual-Level Evidential face forgery Detection (DLED) method employs CLIP (Radford et al., 2021) as the backbone for both the spatial and frequency branches, using the ViT-B/16 (Dosovitskiy, 2020) encoder with half-precision (fp16) data type. The same CLIP configuration is also used for all CLIP-based baseline methods to ensure fair comparisons. For the CLIP Zero-Shot baseline, we used the text prompt “a [CLASS] photo.” as the input, where “[CLASS]” is replaced with the predefined class names corresponding to the seen classes. For CNN-based baseline methods and one-class detectors in Two-stage baselines, all backbones utilize the official implementations provided by the respective authors. These baseline models are trained

054 from scratch for the OSFFD experiments. Specifically, SPSL (Liu et al., 2021) and UCF (Yan
 055 et al., 2023) utilized the Xception backbone (Rossler et al., 2019), while SBI (Shiohara & Yamasaki,
 056 2022) and SIA (Sun et al., 2022) are based on EfficientNet-B4 (Tan & Le, 2019). NPR (Tan et al.,
 057 2024) is a modified version of ResNet (He et al., 2016), and OC-FakeDetect (Khalid & Woo, 2020)
 058 incorporates a Variational Autoencoder. (Kingma & Welling, 2013). Xception (Rossler et al., 2019)
 059 is used directly without modification.

060 **Concrete Implementation.** OSFFD requires the model to simultaneously detect novel fake cat-
 061 egories and perform multiclass classification. Accordingly, we use multiclass classification ac-
 062 curacy (Acc) to evaluate performance on classification, and Detection Rate (DR), defined as the
 063 recall of the unseen fake categories, to assess the model’s ability to discover novel fake. In our
 064 experiments, the batch size was set to 32 for training and 100 for testing across all models. Our
 065 DLED model employed the softplus function as its confidence function $h(\cdot)$. Both DLED and
 066 CLIP-based baseline models are optimized using SGD with a learning rate of 0.002, while the re-
 067 maining baseline methods use the Adam optimizer with a learning rate of $1e^{-4}$. All models, except
 068 for the CLIP Zero-Shot baseline, are trained for 50 epochs. We randomly selected a seed and eval-
 069 uated the model’s performance at the final epoch in a single run. All methods are implemented
 070 in PyTorch, and experiments are conducted on an RTX 6000 Ada GPU. Our code is available at
 071 <https://anonymous.4open.science/r/NovelDFD-BF78>.

072 **AI Disclosure.** We used generative AI to edit portions of this paper for clarity, grammar, and word
 073 choice.

075 C DLED ALGORITHM

077 In this section, we provide a detailed description of the inference procedure for our DLED model.
 078 We denote the spatial and frequency branches as \mathcal{F}^s and \mathcal{F}^f , respectively, such that $\mathcal{F} = \{\mathcal{F}^s, \mathcal{F}^f\}$.
 079 Given the retrieved uncertainty thresholds $\{\tau_k\}_{k=1}^K$ for each known class k , the DLED inference
 080 procedure for an input face image x is described in Algorithm 1, where $h(\cdot)$ denotes the evidence
 081 function and $\text{FFT}(\cdot)$ represents the Fast Fourier Transform.

082 Algorithm 1 DLED Inference Procedure

084 **Require:** Input image x ; uncertainty thresholds $\{\tau_k\}_{k=1}^K$ for each known class.
 085 1: Obtain the frequency map: $x^f = \text{FFT}(x)$
 086 2: Extract dual-level evidence: $e^s = h(\mathcal{F}^s(x))$, $e^f = h(\mathcal{F}^f(x^f))$
 087 3: Calculate belief and uncertainty for each branch:
 088 $b_k = e_k/S, \quad u = K/S, \quad S = \sum_{k=1}^K (e_k + 1)$
 089 4: Fuse belief and uncertainty:
 090 $\tilde{b}_k = \gamma(b_k^s b_k^f + b_k^s u^f + b_k^f u^s),$
 091 $\tilde{u} = \gamma u^s u^f, \quad \gamma = 1 / \left(1 - \sum_{i \neq j} b_i^s b_j^f\right)$ [Eq. 5]
 092 5: Calculate fused evidence and parameters:
 093 $\tilde{S} = K/\tilde{u}, \quad \tilde{e}_k = \tilde{b}_k \times \tilde{S}, \quad \tilde{\alpha}_k = \tilde{e}_k + 1$ [Eq. 6]
 094 6: Calculate predictive distribution and predicted label:
 095 $\tilde{p}_k = \tilde{\alpha}_k/\tilde{S}, \quad \tilde{y} = \arg \max_k \tilde{p}_k$
 096 7: Improve uncertainty estimation:
 097 $\hat{u} = 1 / (\max\{\tilde{\alpha}_1, \dots, \tilde{\alpha}_K\})$ [Eq. 8]
 098 8: Novel category detection and final prediction:
 099 $\hat{y} = \begin{cases} \tilde{y}, & \text{if } \hat{u} \leq \tau_{\tilde{y}} \\ K + 1, & \text{if } \hat{u} > \tau_{\tilde{y}} \end{cases}$
 100 9: **return** \hat{y} and \hat{u}

104 D INFLUENCE OF UNCERTAINTY THRESHOLD

105 In this section, we present additional experimental results analyzing the impact of the uncertainty
 106 threshold on the OSFFD problem. Uncertainty threshold is calculated from the training data such

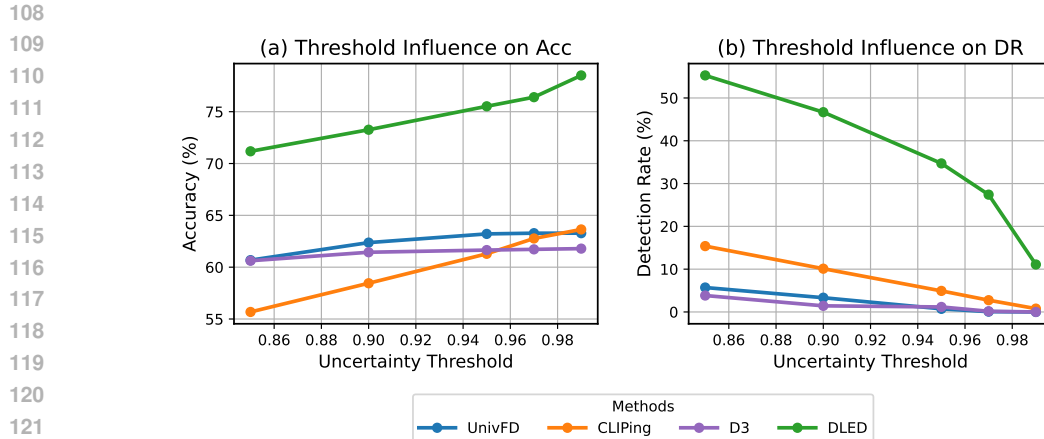


Figure 1: Accuracy and Detection Rate across different uncertainty thresholds for UnivFD, CLIPing, D^3 , and DLED.

that a certain ratio of the samples in each class are marked as known. Our experiments on the OSFFD problem followed the widely adopted open set recognition evaluation protocol (Wang et al., 2022; Zhao et al., 2023), which sets the uncertainty threshold at 95%. A higher threshold indicates that more training samples are regarded as reliable, thereby imposing a stricter criterion for novel fake discovery. To further investigate the impact of the uncertainty threshold on the OSFFD problem, we conducted a series of experiments using various threshold values [0.85, 0.90, 0.95, 0.97, 0.99] on DLED, as well as three CLIP-based baseline methods: UnivFD (Ojha et al., 2023), CLIPing (Khan & Dang-Nguyen, 2024), and D^3 (Yang et al., 2025).

In this experiment, FS and FR are treated as seen fake categories, while EFS is designated as the only novel fake category. The results are presented in Figure 1. It can be observed that as the uncertainty threshold increases, classification accuracy improves, whereas the novel fake discovery rate declines. This indicates that a stricter threshold reduces the detection of novel samples but also decreases the misclassification of known samples. These findings highlight the critical role of the uncertainty threshold in balancing known class classification and novel fake discovery. Moreover, across all threshold settings, our DLED method consistently achieves higher Acc and DR compared to the three CLIP-based baselines, demonstrating its robustness and superior performance.

162 REFERENCES
163

164 Alexey Dosovitskiy. An image is worth 16x16 words: Transformers for image recognition at scale.
165 *arXiv preprint arXiv:2010.11929*, 2020.

166 Kaiming He, Xiangyu Zhang, Shaoqing Ren, and Jian Sun. Deep residual learning for image recog-
167 nition. In *Proceedings of the IEEE conference on computer vision and pattern recognition*, pp.
168 770–778, 2016.

169

170 Yinan He, Bei Gan, Siyu Chen, Yichun Zhou, Guojun Yin, Luchuan Song, Lu Sheng, Jing Shao, and
171 Ziwei Liu. Forgerynet: A versatile benchmark for comprehensive forgery analysis. In *Proceed-
172 ings of the IEEE/CVF conference on computer vision and pattern recognition*, pp. 4360–4369,
173 2021.

174 Hasam Khalid and Simon S Woo. Oc-fakedect: Classifying deepfakes using one-class variational
175 autoencoder. In *Proceedings of the IEEE/CVF conference on computer vision and pattern recog-
176 nition workshops*, pp. 656–657, 2020.

177

178 Sohail Ahmed Khan and Duc-Tien Dang-Nguyen. Clipping the deception: Adapting vision-
179 language models for universal deepfake detection. In *Proceedings of the 2024 International
180 Conference on Multimedia Retrieval*, pp. 1006–1015, 2024.

181 Diederik P Kingma and Max Welling. Auto-encoding variational bayes. *arXiv preprint
182 arXiv:1312.6114*, 2013.

183

184 Honggu Liu, Xiaodan Li, Wenbo Zhou, Yuefeng Chen, Yuan He, Hui Xue, Weiming Zhang, and
185 Nenghai Yu. Spatial-phase shallow learning: rethinking face forgery detection in frequency do-
186 main. In *Proceedings of the IEEE/CVF conference on computer vision and pattern recognition*,
187 pp. 772–781, 2021.

188 Utkarsh Ojha, Yuheng Li, and Yong Jae Lee. Towards universal fake image detectors that generalize
189 across generative models. In *Proceedings of the IEEE/CVF Conference on Computer Vision and
190 Pattern Recognition*, pp. 24480–24489, 2023.

191

192 Alec Radford, Jong Wook Kim, Chris Hallacy, Aditya Ramesh, Gabriel Goh, Sandhini Agarwal,
193 Girish Sastry, Amanda Askell, Pamela Mishkin, Jack Clark, et al. Learning transferable visual
194 models from natural language supervision. In *International conference on machine learning*, pp.
195 8748–8763. PMLR, 2021.

196

197 Andreas Rossler, Davide Cozzolino, Luisa Verdoliva, Christian Riess, Justus Thies, and Matthias
198 Nießner. Faceforensics++: Learning to detect manipulated facial images. In *Proceedings of the
199 IEEE/CVF international conference on computer vision*, pp. 1–11, 2019.

200

201 Kaede Shiohara and Toshihiko Yamasaki. Detecting deepfakes with self-blended images. In *Pro-
202 ceedings of the IEEE/CVF Conference on Computer Vision and Pattern Recognition*, pp. 18720–
203 18729, 2022.

204

205 Ke Sun, Hong Liu, Taiping Yao, Xiaoshuai Sun, Shen Chen, Shouhong Ding, and Rongrong Ji. An
206 information theoretic approach for attention-driven face forgery detection. In *European Confer-
207 ence on Computer Vision*, pp. 111–127. Springer, 2022.

208

209 Chuangchuang Tan, Yao Zhao, Shikui Wei, Guanghua Gu, Ping Liu, and Yunchao Wei. Rethinking
210 the up-sampling operations in cnn-based generative network for generalizable deepfake detection.
211 In *Proceedings of the IEEE/CVF Conference on Computer Vision and Pattern Recognition*, pp.
212 28130–28139, 2024.

213

214 Mingxing Tan and Quoc Le. Efficientnet: Rethinking model scaling for convolutional neural net-
215 works. In *International conference on machine learning*, pp. 6105–6114. PMLR, 2019.

216

217 Haoqi Wang, Zhizhong Li, Litong Feng, and Wayne Zhang. Vim: Out-of-distribution with virtual-
218 logit matching. In *Proceedings of the IEEE/CVF conference on computer vision and pattern
219 recognition*, pp. 4921–4930, 2022.

216 Zhiyuan Yan, Yong Zhang, Yanbo Fan, and Baoyuan Wu. Ucf: Uncovering common features for
217 generalizable deepfake detection. In *Proceedings of the IEEE/CVF International Conference on*
218 *Computer Vision*, pp. 22412–22423, 2023.

219
220 Zhiyuan Yan, Taiping Yao, Shen Chen, Yandan Zhao, Xinghe Fu, Junwei Zhu, Donghao Luo,
221 Chengjie Wang, Shouhong Ding, Yunsheng Wu, et al. Df40: Toward next-generation deepfake
222 detection. *arXiv preprint arXiv:2406.13495*, 2024.

223 Yongqi Yang, Zhihao Qian, Ye Zhu, Olga Russakovsky, and Yu Wu. D[^] 3: Scaling up deepfake
224 detection by learning from discrepancy. In *Proceedings of the Computer Vision and Pattern*
225 *Recognition Conference*, pp. 23850–23859, 2025.

226 Chen Zhao, Dawei Du, Anthony Hoogs, and Christopher Funk. Open set action recognition via
227 multi-label evidential learning. In *Proceedings of the IEEE/CVF Conference on Computer Vision*
228 *and Pattern Recognition (CVPR)*, pp. 22982–22991, June 2023.

230

231

232

233

234

235

236

237

238

239

240

241

242

243

244

245

246

247

248

249

250

251

252

253

254

255

256

257

258

259

260

261

262

263

264

265

266

267

268

269